Evaluation of Shear Performance of Timber-Timber Composite Joints

Yo-Jin Song,[a] Seong-Yeob Baek,[b] and Soon-Il Hong [b,*]

The mechanical performance of timber composite floors is influenced by the degree of composite action between the components. In this study, the shear strength performance of cross-laminated timber and glued laminated timber composite floors based on the joining method was evaluated by push-out test. Eight types of timber-timber composite joints were evaluated using three different methods: lag screw joints, glued-in rod joints using fully threaded bolts and glass fiber reinforced plastic, and hybrid joints. Strength characteristics were derived to make theoretical predictions on the load-carrying capacity of the joints. The results showed that the glued-in rod joints were superior to the lag screw joints, with slip coefficients and ductility measured as 10 times and 2.5 times higher, respectively. The reliability of the strength characteristics of the glued-in rod joints was remarkably different depending on the presence or absence of anti-adhesive tape applied to the timber-to-timber joint surface. The load capacity of the hybrid joint, which combines mechanical and glued-in rod joining methods, was 47% higher than that of the lag screw joint and 38% higher than that of the glued-in bolt joint. In the European Yield Model modified to estimate the load capacity of joints, the rope effect and the yield moment of the fasteners had a remarkable impact on the predicted load capacity.

*Contact information: a: Institute of Forest Science, Kangwon National University, Chun-Cheon 200-701 Republic of Korea; b: Department of Forest Biomaterials Engineering, Kangwon National University, Chun-Cheon 200-701 Republic of Korea; *Corresponding author: hongsi@kangwon.ac.kr*

INTRODUCTION

Using wood is increasingly recognized as a sustainable alternative in construction, in line with national carbon reduction policies. Engineered wood products, such as cross-laminated timber (CLT) and glued laminated timber (glulam), are known for their high specific strength, which makes them easy to handle during construction and allows for a high level of prefabrication (Izzi *et al*. 2018). Despite these advantages, timber floors have difficulty spanning unsupported lengths due to the relatively low modulus of elasticity of wood compared to concrete and steel. Increasing the thickness of the slab, such as CLT, is the easiest solution to control deflection and vibration, but excessive increases in slab thickness are not economically and structurally efficient. Hence, researchers have attempted to extend the span of timber floors over the past few years with studies on steel-timber composite (STC), timber-concrete composite (TCC), and timber-timber composite (TTC) floors (Hassanieh *et al*. 2017; Baek *et al*. 2021; Nie and Valipour 2022; Owolabi

bioresources.cnr.ncsu.edu

and Loss 2022; Song *et al.* 2022). In particular, TTC floors use more wood than STC or TCC floors. In addition, TTC flooring can also reduce the use of steel or concrete, which can significantly reduce the self-weight of the structure. The structural performance of timber-timber composite flooring is strongly influenced by the mechanical properties of the shear joints between the slab and the beam (or joist) (Nie *et al.* 2021). Therefore, in research on composites, the joint performance and behavior are usually analyzed through push-out tests on symmetrical joints, and the structural performance of the composite floor is predicted and analyzed through theoretical and finite element models based on the joint test results. In this process, the bending strength of the fasteners, the embedment strength of the wood, and the pullout strength are evaluated to derive strength properties for modeling because researchers have confirmed that the strength of TTC shear joints significantly impacts the maximum load-carrying capacity of TTC floors.

Research on joints has been mainly focused on mechanical joints with screws or bolts, and less frequently, glued-in rod joints, where holes are drilled in the timber to insert bolts or steel rods and filled with adhesive or grout. These have been studied, but not enough (Yagi *et al*. 2016; Chiniforush *et al*. 2021; Hammad *et al*. 2022; Zhang *et al*. 2023). Adhesive joints are considered to have very high load capacity and stiffness. However, their high brittleness and unreliable joint behavior are reasons that mechanical joints, such as nails, screws, or dowel-type fasteners, are often chosen for TTC joints instead.

This study evaluated the shear performance of CLT-GLT composite joints with lag screw joint, glued-in dowel joint, and hybrid joint. Eight types of TTC joints were tested for push-out strength based on the type of timber joint, depth of lag screw penetration, the diameter of the fully threaded bolt, diameter, and presence of threads on the GFRP rod. Additionally, a report on the improved constructability of the glued-in dowel method was included. Strength characteristics derived from embedment tests on the fastener's shear strength and timber materials (CLT and GLT) were compared between a model applying the European Yield Model (EYM) and a model applying the formulas of Eurocode 5 (EN1995-1-1 2010). The estimated load capacity and slip coefficient of the models applying EYM were compared with the results of push-out tests.

EXPERIMENTAL

Material Properties
CLT and GLT

Both CLT and GLT were fabricated from kiln-dried larch (*Larix kaempferi* (Lamb.) Carr.) lumber. The average air-dried specific gravity and average air-dried moisture content of the larch lumber pieces were 0.57 (S.D: 0.05) and 11.9% (S.D: 1.4), respectively, and their dimensions were 30 mm (t) × 120 mm (w). The GLT, the beam element of the CLT-GLT composite floor, was laminated in eight layers, and its strength class was 10S-30B (symmetrical combination) according to KS F 3021 (2018). The floor element, CLT, was laminated in five layers and had a strength class of C-E12-E10 (E12 for the longitudinal layer, E10 for the horizontal layer) according to KS F 2081 (2021). Both timbers were laminated with phenol-resorcinol formaldehyde adhesive (PRF). Timber dimensions and density (ρ), moisture content (MC), bending strength (f_b), and elastic modulus (E) are shown in Table 1.

Table 1. Mechanical Properties of GLT and CLT (Bending strength and elastic modulus are characteristic values)

Timber type	Grade	Size $t \times w \times l$ (mm)	ρ (kg/m³)	f_b (MPa)	E (GPa)
GLT	10S-30B	240 × 120 × 700	531.0 ± 14.4	30.0	10.0
CLT	C-E12-E10	600 × 350 × 150	599.2 ± 4.5	28.6	9.6

Fastener

Six different types of fasteners were used in the CLT-GLT joint, including lag screws, fully threaded bolts, and glass fiber-reinforced plastic (GFRP), depending on the diameter, length, and threaded or unthreaded, as illustrated in Fig. 1(a). Lag screws were used in lengths of 200 and 250 mm with a diameter of 10 mm. Fully threaded bolts were used in diameters of 10 and 12 mm and length of 250 mm. The GFRP rods had the same diameter and length of 12 and 250 mm, respectively, threaded or not. The bending tests on them were performed with a three-point load, as indicated in Fig. 1(b). The yield load $F_{y,5\%}$ was determined by the 5% offset method, and the yield moment M_y was calculated from $F_{y,5\%}$. The plastic yield moment M_P was estimated using the following equation for the plastic cross-sectional modulus s,

$$s = \frac{1}{6}(1.1d_{in})^3 \qquad (1)$$

where d_{in} is the fastener's root diameter. Table 2 summarizes the bending strength characteristics of the fasteners.

(a)   **(b)**

Fig. 1. Mechanical fasteners and setup of three-point bending test

Table 2. Characteristics of Bending Strength of the Fasteners

Fastener Type	Size $d \times l$ (mm)	Root Diameter (mm)	$F_{y,5\%}$ (N)	M_y (Nm)	M_P (Nm)
Lag screws	10 × 200	6.6	380.6	31.1	24.2
	10 × 250	7.7	587.0	48.0	59.2
Fully threaded bolts	10 × 250	8.5	740.6	60.6	100.5
	12 × 250	9.6	995.2	168.8	194.5
Non-threaded GFRP rod	12 × 250	12.0	1005.8	170.6	384.0
Fully-threaded GFRP rod	12 × 250	11.9	889.1	150.8	331.0

Push-out Test of CLT-GLT Joints

Configuration of CLT-GLT joints

The push-out specimens for the shear strength evaluation of CLT-GLT joints were made of eight types, as presented in Fig. 2. The specimens consisted of a symmetrical structure (CLT-GLT-CLT) with two CLT slabs and one GLT beam joined by four fasteners to ensure uniform load transfer and avoid eccentric loads at the joints. The distance between the fasteners was 300 mm. The end distance, edge distance, and spacing of the fasteners satisfied ETA-11/0190 (DIBT 2013).
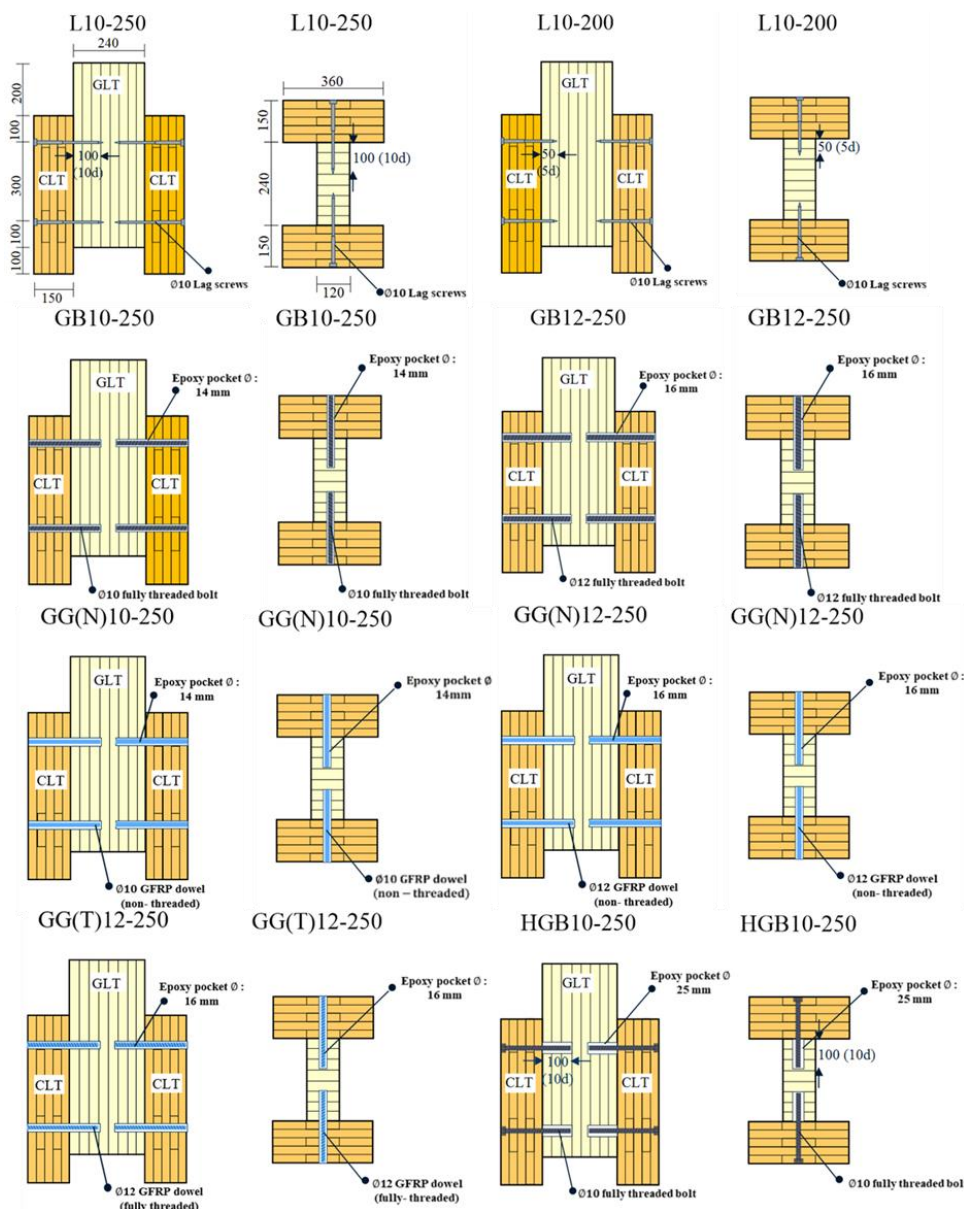

Fig. 2. Outline of geometry, dimensions (all dimensions in mm), and configuration of the CLT-GLT push-out specimens

The specimens were made from three jointing methods: mechanical joint (L10) by lag screws, glued-in rod joint (GB, GG) in which a dowel-type fastener was inserted by

machining a hole in the joint and filling the gap between the hole and the dowel with glue, and hybrid method (HGB) in which a glued in rod joint was constructed using fully threaded bolts on the GLT beam, and a nut was used on the CLT floor. In the case of lag screw joints, the CLT and GLT were pre-drilled 2 mm smaller than the diameter of the lag screws to prevent breakage of the lag screws and misalignment of the GLT beams during the process of joining the CLT and GLT. For the glued-in rod joints, the holes drilled in the CLT and GLT were 4 mm larger than the diameter of the dowel and filled with epoxy (adhesive layer: 2 mm). For some of the specimens (GB10-250-3 and 4, GB12-250-3 and 4, GG(N)10-250, GG(T)12-250) with glued-in rod joints, anti-adhesive tape was applied to the contact surface of the CLT and GLT to prevent the CLT and GLT from being bonded by the adhesive that leaked out during adhesive filling (*i.e.*, to prevent adhesive bonding behavior during the push-out test). For the hybrid method, a hole with a diameter of 25 mm and a depth of 10 d (d: diameter of the dowel) was machined in the GLT and filled with adhesive, and a hole 2 mm larger than the diameter of the fully threaded bolt was machined in the CLT to improve the constructability of the joint installation. In the specimen naming convention, the first part (before -) refers to the type and diameter of the fastener, and for GFRP rods, information about the presence or absence of threads is included in parentheses. The second part (after -) indicates the length of the fastener, and the third part (after the second -) represents the number of repetitions. More information about the push-out specimens is given in Table 3.

Table 3. Designation, Nominal Geometry/Dimensions of the Fasteners, and Details of the TTC Joints

Specimens	Shear Connector		CLT Panel	GLT beam	No. Repeats
	Type	Size: $d \times l$ (mm)	Size: $h \times w \times l$ (mm)		
L10-200	Lag screw	10 × 200	150 × 350 × 600	240 × 140 × 700	3
L10-250	Lag screw	10 × 250	150 × 350 × 600	240 × 140 × 700	3
GB10-250	Glued in FB	10 × 250	150 × 350 × 600	240 × 140 × 700	4
GB12-250	Glued in FB	12 × 250	150 × 350 × 600	240 × 140 × 700	4
GG(N)10-250	Glued in NG	10 × 250	150 × 350 × 600	240 × 140 × 700	2
GG(N)12-250	Glued in NG	12 × 250	150 × 350 × 600	240 × 140 × 700	2
GG(T)12-250	Glued in FG	12 × 250	150 × 350 × 600	240 × 140 × 700	3
HGB10-250	Hybrid	10 × 250	150 × 350 × 600	240 × 140 × 700	3
Note: FB: fully threaded bolt, NG: non-threaded GFRP, FG: fully threaded GFRP					

Instrumentation and loading procedure

Push-out tests on CLT-GLT joints were performed in a vertical load-testing machine with a maximum capacity of 300 kN. The load was applied to a cross-section of the GLT, with the direction of the load parallel to the fiber direction of the GLT. The slip between CLT and GLT was measured using two displacement transducers (CDP-50,

Tokyo Sokki Kenkyujo, Japan) installed at the same height as the fasteners at the front and back of the joint, as detailed in Fig. 3. The loading protocol for the test was divided into two phases according to EN 26891 (1991) (Fig. 4). In the first step, the specimen was loaded to 40% of the expected maximum load for the first 120 s, and the load was held for 30 s. The load was then reduced from 40% to 10% of the expected maximum load and held for another 30 s. In the second step, the specimen was reloaded until failure. Based on the test results, the maximum load values for subsequent specimens were modified and, if necessary, the loading procedure was redefined.
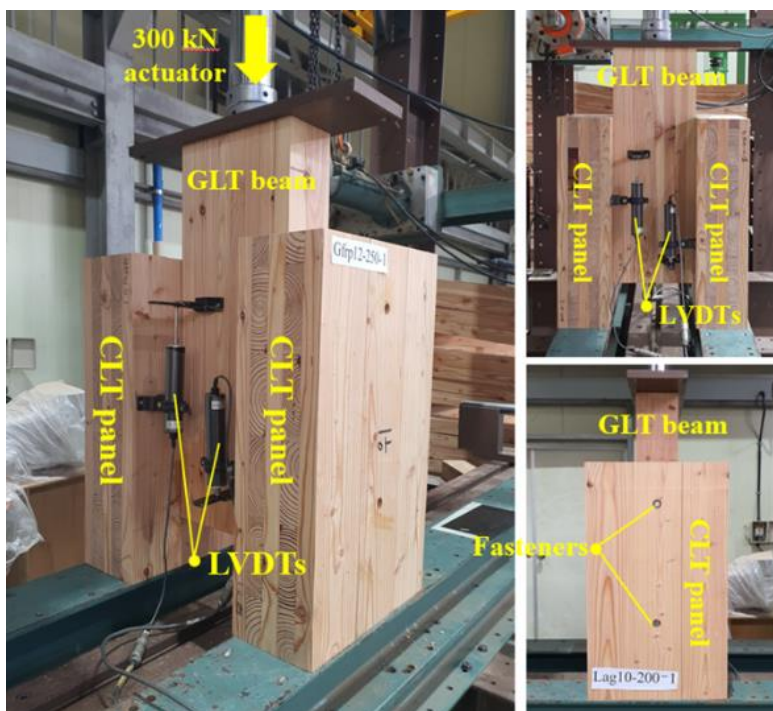

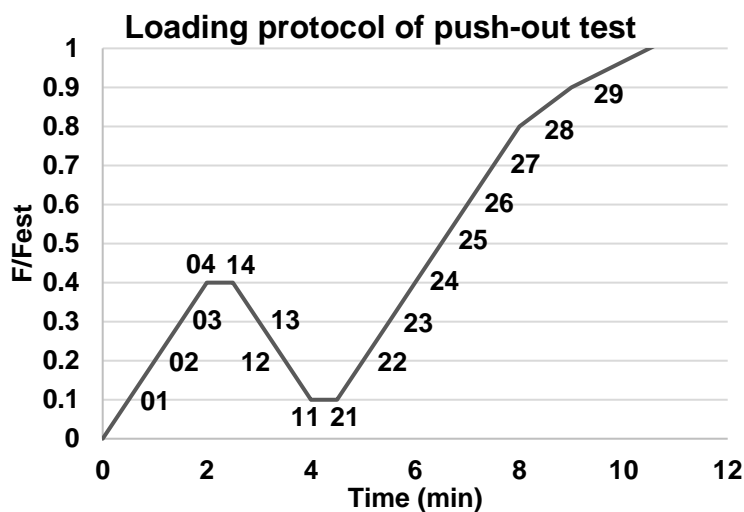**Fig. 3.** Outline of the push-out test setup

Fig. 4. Loading protocol of push-out test (BS EN 26891 1991)

Embedment Tests

Specimens

Eight types of embedment test specimens (two for each type of specimen) were fabricated, as enumerated in Table 4, depending on the type of timber (CLT, GLT), jointing method, and fastener type and size. The specimens were half-hole type according to ASTM D5764 (2007). The glued-in rod specimens had a 2-mm-thick epoxy adhesive layer between the timber and the fastener, while the hybrid specimens had a 7.5-mm-thick adhesive layer between the GLT and the bolt. In the specimen naming convention, the first part (before -) refers to the timber type, and the second part (after -) is the bonding method and the diameter of the fastener.

Table 4. Details of the Specimens and Size of Fasteners in Embedment Tests

Specimens	Timber Type	Timber Size $h \times w \times l$ (mm)	Shear Connector	Diameter of Fastener (mm)	Orientation of Road with Respect to Grain
GLT-L10	GLT	100×120×120	Lag screw	10	Parallel
GLT-GB10			Glued in FB	10	
GLT-GB12			Glued in FB	12	
GLT-GG10			Glued in NG	10	
GLT-HGB10			Hybrid	10	
CLT-L10	CLT	100×120×150	Lag screw	10	
CLT-GB10			Glued in FB	10	
CLT-GB12			Glued in FB	12	
Note: FB: fully threaded bolt, NG: non-threaded GFRP					

Test setup and procedure

The embedment strength test was performed according to ASTM D5764 (2007), with the crosshead applying force to a fastener placed over the half-hole at a speed of 1 mm/min. The direction of the load was parallel to the fiber direction of the GLT and CLT (relative to the outermost layer). The yield load was determined by the 5% offset method, and the embedment strength was calculated from Eq. 2 below,

$$f_{h,5\%} = \frac{F_{y,5\%}}{dt} \tag{2}$$

where $f_{h,5\%}$ is the embedment strength (MPa), $F_{y,5\%}$ is the 5% yield load (kN), d is the diameter of fastener (mm), and t is the thickness of timber (mm). The theoretical embedment strength, $f_{h,EC5}$, suggested by Eurocode 5 (EN 1995-1-1 2010), was estimated using the following Eq. 3,

$$f_{h,EC5} = \frac{0.082(1-0.01d)\rho_m}{k_{90}\sin^2\alpha + \cos^2\alpha} \tag{3}$$

where d is the diameter of the fastener (mm), and ρ_m is the density of timber (kg/m^3), α is the penetration angle of the fastener with respect to the grains, k_{90} is a correction factor that depends on the type of timber.

RESULTS AND DISCUSSION

Push-out Test Results

Failure mode

Fasteners in CLT-GLT joints were subjected to a single shear load, and six failure modes can be categorized according to the embedment strength of the CLT and GLT, the size and strength of the fastener, the thickness of the CLT, and the fastener embedment length in the GLT. Failure modes I and II were related to the embedment of the CLT or GLT around the fastener without significant plastic deformation of the shear fastener. In the case of glued-in rod joints, the epoxy adhesive layer of the CLT or GLT was destroyed. Failure mode III involved the embedment of CLT and GLT (or epoxy adhesive layer). Failure modes IV and V resulted in a single plastic hinge in the shear fastener, while failure mode VI resulted in two plastic hinges in the shear fastener. Reportedly, failure modes I through III were associated with brittle failure, while failure modes IV through VI were categorized as ductile failure (Chiniforush *et al.* 2021). In addition, for adhesive bonding, the brittle failure of the adhesive layer affects the brittle behavior of the joint (Nie *et al.* 2021). When the penetration depth of the lag screw in the GLT was 10 d (100 mm) (L10-250), two plastic hinges were observed in the fastener, which corresponded to failure mode VI, and when the penetration depth was shortened to 5 d (50 mm) (L10-200), it was related to failure mode IV or V. In the glued-in bolt joints (GB10-250, GB12-250) and hybrid joints (HGB10-250), a plastic hinge occurred in the bolt after the adhesive layer was destroyed. These joints were subjected to failure mode VI regardless of the diameter of the bolt or the thickness of the adhesive layer. Glued-in GFRP rod joints (GG(N)10-250, GG(N)12-250, GG(T)12-250) were also associated with failure mode VI. Most of these joints saw the GFRP cut due to increased slip after the maximum load, which was observed more in the threaded GFRP (GG(T)12-250). For the unthreaded GFRP rod, the slip of the joint increased, as it was easily pulled out of the timber by the low bond shear strength with the adhesive layer.
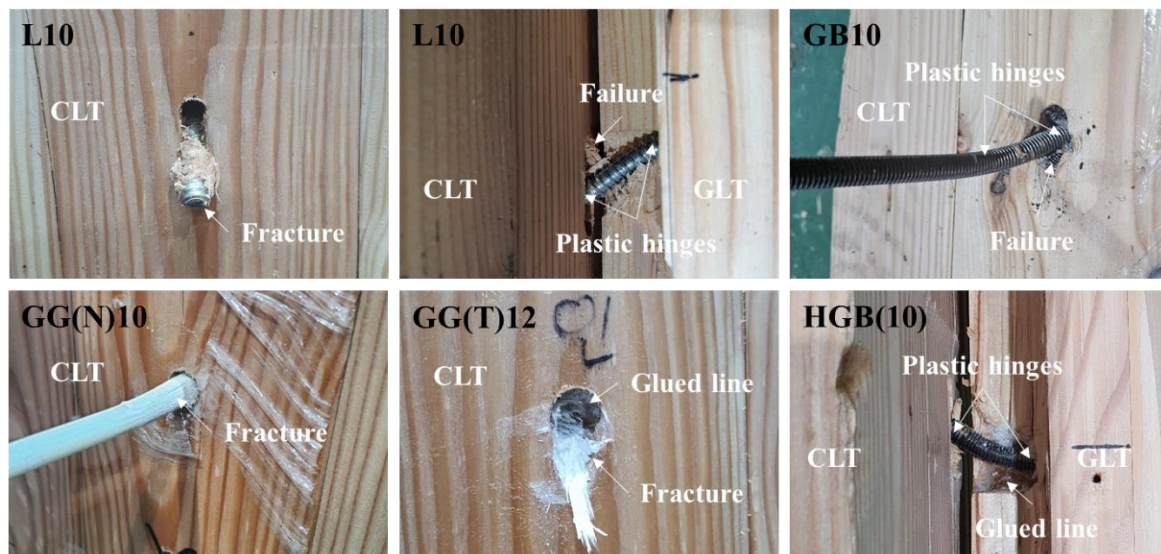

Fig. 5. Failure modes of TTC joints

Load-slip behavior

The load-slip curve for the push-out test is shown in Fig. 6. The slip in the load-slip curve is the average value of the strain measured by the four displacers. The behavior of the load-slip curves for the lag screw joint specimens was close to bilinear. The specimens with glued-in rod joints without anti-adhesive tape (GB10-250-1 and 2, GB12-250-1 and 2, GG(N)12-250) exhibited a near linear load-slip behavior with little slip up to the maximum load, after which the load dropped remarkably due to the breakdown of the adhesive layer between the two timber surfaces. This brittle behavior has been commonly observed in adhesive joints (Nie *et al.* 2021; Hammad *et al.* 2022), which suffer from inconsistent load-slip behavior. In contrast, the load-slip curves of glued-in rod joints with anti-adhesive tape (GB10-250-3 and 4, GB12-250-3 and 4, GG(N)10-250, and GG(T)12-250) were similar to those of lag screw joints. The test results revealed that applying anti-adhesive tape could induce a constant load-slip behavior of the joint. For the hybrid joint (HGB10-250), the load-slip behavior was close to bilinear without any tape application.
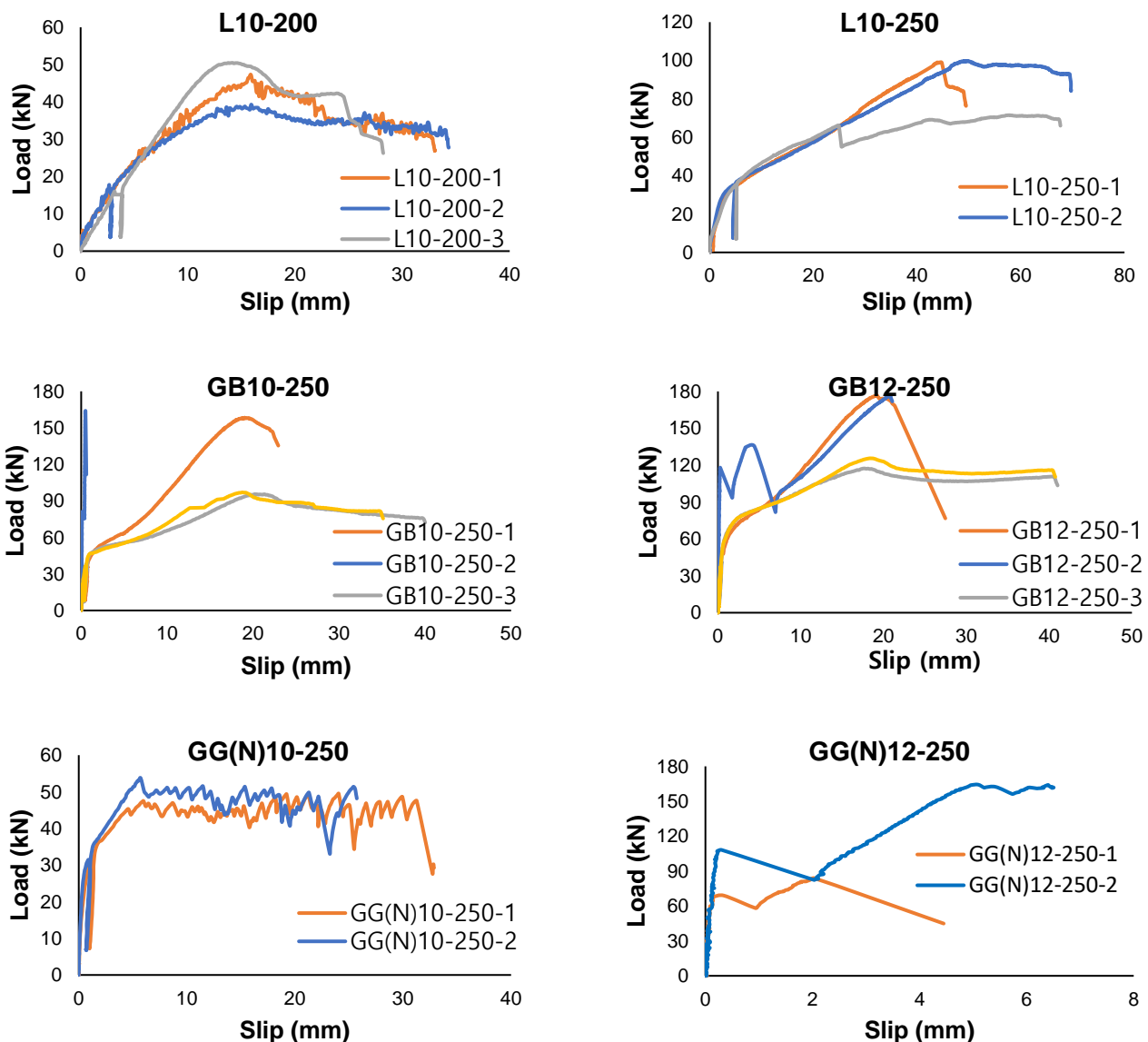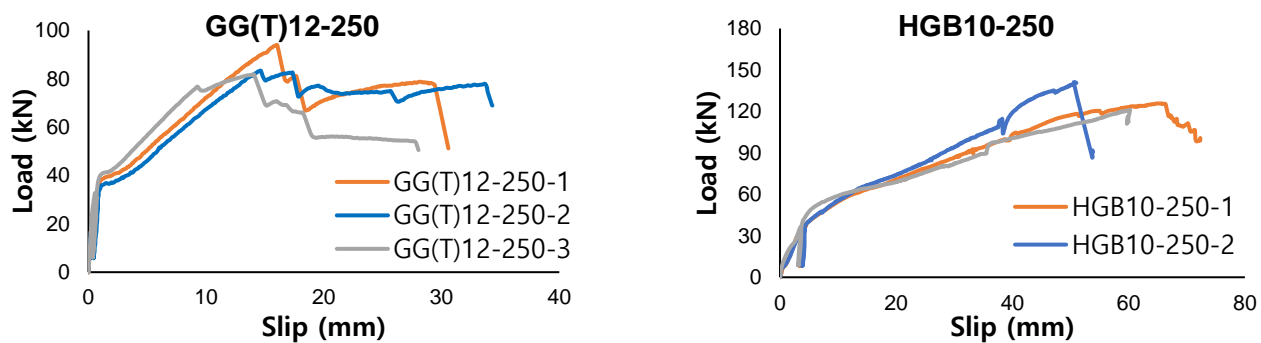
Fig. 6. Load-slip curves of CLT-GLT composite joints

Strength and slip modulus (K_s)

The maximum shear load and yield load of the joints, along with their corresponding displacements, as well as the slip coefficient and ductility index, are reported in Table 5. Various methods have been proposed to determine the yield strength characteristics of the joint (Muñoz *et al.* 2008). The values on the load-slip curve obtained from experimental tests were determined using the Yasumura and Kawai (Y&K) and 5% offset methods (Yasumura 1998). Among them, the 5% offset method was not suitable for determining the yield strength for specimens with adhesive bonding behavior, so the Y&K yield strength determination method was finally used.

The parameter K_s, which remarkably impacts the short-term settlement of CLT-GLT composite floor structures, was calculated using the following equation, through a straight line with a slope penetrating between 10% and 40% of F_{max} on the load-slip curve (EN-26891 1991),

$$K_s = \frac{0.4F_{max} - 0.1F_{max}}{v_{0.4} - v_{0.1}}$$ (4)

where $0.1F_{max}$ and $0.4F_{max}$ are 10% and 40% of F_{max}, and $v_{0.1}$ and $v_{0.4}$ are slips corresponding to $0.1F_{max}$ and $0.4F_{max}$.

The ductility of the joint was quantified using Eq. 5, as reported by Smith *et al.* (2006),

$$\mu = v_{max}/v_y$$ (5)

where μ is a ductility index, v_{max} is a slip corresponding to F_{max}, and v_y is a slip corresponding to F_y that was determined by the above-mentioned Y&K method. According to Smith *et al.* (2006), it is classified as ductile if the ductility index $\mu > 6$ and brittle if $\mu < 2$.

For the lag screw joint, when the penetration depth into the GLT was 5 d, the average F_{max} was 45.7 kN. Increasing the penetration depth of GLT to 10 d resulted in a 97% increase in the average F_{max} to 90.2 kN. The increase in penetration depth resulted in a 31% increase in K_s and improved the ductility of the joint.

Joints without applied anti-adhesive tape may exhibit a very high F_{max}, making them appear as superior joints. However, due to minimal slip, it was extremely challenging to derive strength characteristics from the load-slip curve. Within the same type of joint,

the variation in slip response to loads was remarkable, depending on the test specimen, resulting in low reliability of strength characteristics. Anti-adhesive tape considerably reduced the effect of load increase due to adhesive bonding, resulting in a relatively lower F_{max} measurement while increasing the reliability of the derived strength characteristics. Therefore, the analysis of the glued-in rod joints described below compared specimens where the anti-adhesive tape was not applied.

Comparing fasteners of the same diameter confirmed that the glued-in bolt joint method could increase the K_s of the CLT-GLT joint over 10 times in GB10-250 and L10-250. The joint exhibited a very high ductility level. Increasing the diameter of the bolt from 10 to 12 mm resulted in a 24% increase in average F_{max} and a 41% increase in K_s, confirming that increasing the diameter effectively enhances the joint's performance, which contradicts the common belief that bonding by adhesives leads to high strength but low ductility (Hassanieh *et al.* 2017).

The reliability of the strength characteristics of joints using GFRP rods, namely GG(N)12-250, was low due to adhesive failure. Comparing the performance of joints based on the increase in diameter of GFRP rods was deemed impractical. Increasing the diameter of the GFRP rod from 10 mm to 12 mm and adding a threaded insert to the GG(T)12-250 resulted in a 70% increase in F_{max}, but K_s decreased 42%, which did not effectively enhance the performance of the joint, contrasting with the results of joints using bolts. Nevertheless, GG(T)12-250 was still effective in the composite of CLT-GLT because of its higher K_s and μ compared to L10-250.

The average F_{max} of GB12-250 was 121.4 kN, while the average F_{max} of GG(T)12-250 was 86.3 kN, implying that the bolt exhibited 41% higher shear performance. In the glued-in rod jointing method, using bolts increased K_s 178% compared to GFRP rods. This outcome is closely related to the difference in strength (MOR and MOE) between bolts and GFRP rods.

The average F_{max} of the hybrid joint was measured at 132.7 kN, the highest among the glued-in rod joints tested, except for the specimen where the adhesive failure occurred. This is an average F_{max} that is 47% higher than the L10-250 joint with lag screw of the same diameter, and 38% higher than the GB10-250 joint with glued-in bolt. Considering the challenging nature of constructing glued-in rod joints, hybrid construction methods can be a rational choice for improving the constructability of CLT-GLT composite floors. However, the hybrid method exhibited minimal impact on the joint's K_s and ductility. In the case of K_s, the loose clearance between the bolt hole in the timber and the bolt diameter, as well as increased slip at the joint, were suspected to cause the bolt head to easily be sucked into the CLT interior, leading to destruction modes. The ductility of the bonding area did not improve due to the increased brittleness in proportion to the thickened adhesive layer.

Table 5. Characteristic of CLT-GLT for Push-out Test

Specimens	Anti-adhesive Tape	F_{max} (kN)	v_{max} (mm)	F_y (kN)	v_y (mm)	k_s (kN/mm)	μ
L10-200-1	-	47.3	15.9	21.7	4.1	4.7	3.9
L10-200-2	-	39.3	15.9	18.7	3.0	5.5	5.3
L10-200-3	-	50.5	13.8	20.8	4.5	4.2	3.1

L10-250-1	-	99.2	44.6	39.7	7.6	4.3	5.9
L10-250-2	-	99.8	49.9	39.9	7.1	7.6	7.0
L10-250-3	-	71.5	58.0	37.5	5.8	7.1	10.1
GB10-250-1	X	158.4	18.8	46.1	9	10.4	2.1
GB10-250-2	X	164.1	0.5	78	0.1	787.4	5
GB10-250-3	O	95.6	21.3	47.1	1.1	71.5	19.4
GB10-250-4	O	97	18.8	46	1	86.1	18.8
GB12-250-1	X	176.6	19.2	70.7	2.1	27.2	9.1
GB12-250-2	X	177.1	20.8	118.1	0.2	634.5	104.2
GB12-250-3	O	117.1	17.6	68	1.3	125.7	13.6
GB12-250-4	O	125.6	18.3	68.8	1.4	96.6	13.1
GG(N)10-250-1	O	47.5	6	35	1.6	71.3	3.8
GG(N)10-250-2	O	53.8	5.7	35	1.3	62	4.4
GG(N)12-250-1	X	83.9	2	68.5	1.2	74.5	1.6
GG(N)12-250-2	X	164.3	5.1	100.2	0.8	938.8	6.1
GG(T)12-250-1	O	93.9	16	38.4	1	42.1	16
GG(T)12-250-2	O	83.3	14.6	35	1	31.3	14.6
GG(T)12-250-3	O	81.7	13.9	38	0.8	46.4	17.4
HGB10-250-1	-	125.9	65.7	54.2	9	7.6	7.3
HGB10-250-2	-	140	50.5	58.7	10	6.4	5
HGB10-250-3	-	132.1	60.3	60	16.8	8.1	5.6

Embedment Test Results

Failure mode

Regardless of the timber type, most specimens showed cleavage in the direction of the fibers in the outermost layer because the direction of the fastener embedment load was parallel to the direction of the fibers in the timber. Despite the epoxy glued line in the glued-in rod joint being destroyed by the embedment of the bolt, the bolt successfully transmitted the embedment load to the timber. This destructive mode manifested as ductile behavior, as reflected in Fig. 7. A thin adhesive layer with a thickness of 2 mm had little impact on the load-displacement behavior of the material upon failure. Specimens with adhesive layers showed steeper curves compared to specimens without adhesive layers, such as GLT-L10 and CLT-L10 in embedment tests. However, for GLT-HGB10 with an adhesive layer thickness of 7.5 mm, both adhesive layer cracking and timber cleavage occurred simultaneously at F_{max} on the load-displacement curve, which indicates that the timber failed due to embedment by the adhesive layer, unlike the test specimens with a thin adhesive layer that failed due to embedment by the bolt. GLT-GG12 experienced compression failure of the GFRP rod before the epoxy adhesive layer was destroyed or the timber cleavage occurred, preventing the embedment load from being fully transferred to the timber.
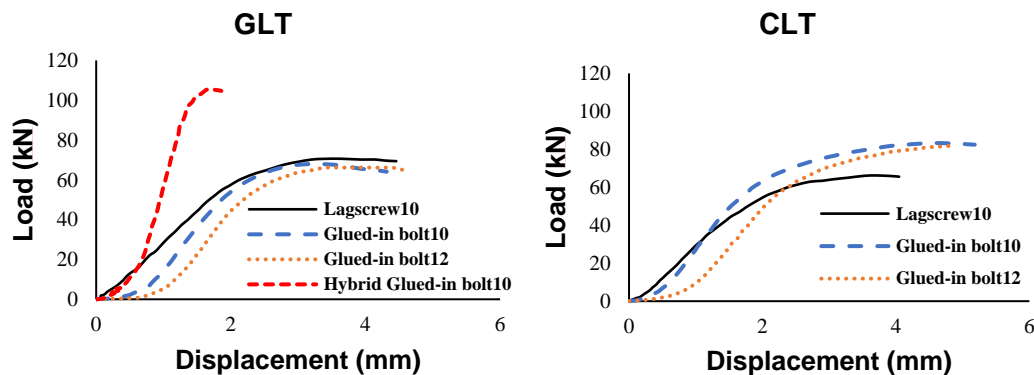
Fig. 7. Failure mode

Fig. 8. Average load-displacement curves of embedment tests

Embedment strength

Table 6 presents the experimental embedment strength $f_{h,5\%}$, theoretical embedment strength $f_{h,EC5}$ calculated by the Eurocode 5 formula, and the ductility index μ (EN 1995-1-1 2010). As explained in the destructive mode, the GFRP test specimen failed due to the fracture of the GFRP rod before the load was transferred to the timber. It should be noted that no embedment strength test was conducted for the CLT. There was no remarkable difference in embedment strength between the lag screw joint and the glued-in bolt joint. The adhesive layer in the glued-in bolt joint reduced the joint's ductility. An increase in bolt diameter at the glued-in bolt joint decreased the embedment strength in GLT and CLT. This finding has also been reported in mechanical joints formed by screws, not just in glued-in rod joints (Sawata and Yasumura 2002). The embedment strength of the Hybrid method (GLT-HGB10) was 48% and 51% higher compared to GLT-L10 and GLT-GB10, respectively. The test results demonstrated that a sufficient thickness of the adhesive layer effectively increased the initial stiffness and maximum load. However, the thick adhesive layer was ineffective in increasing the ductility of the joint.

Table 6. Characteristics of CLT-GLT for the Embedment Test

Specimens	$f_{h,5\%}$ (MPa)	$f_{h,EC5}$ (MPa)	F_{max} (kN)	D_{max} (mm)	$F_{y,5\%}$ (kN)	D_y (mm)	μ
GLT-L10	56.8	26.1	73.0	4.0	68.2	2.7	1.5
GLT-GB10	55.4	26.1	68.6	3.4	66.5	2.8	1.2
GLT-GB12	45.5	38.3	66.9	3.6	65.6	3.1	1.2
GLT-GG12	46.8	-	67.9	3.7	67.4	3.4	1.1
GLT-HGB10	83.8	57.6	100.5	2.7	100.5	2.6	1.0
CLT-L10	40.5	29.5	69.1	5.3	60.7	2.45	2.2
CLT-GB10	48.6	29.5	85.7	5.3	73.0	2.5	2.1
CLT-GB12	42.8	28.3	83.7	5.1	77.0	3.3	1.5

$f_{h,5\%}$: Experimental embedment strength, $f_{h,EC5}$: Theoretical embedment strength, F_{max}: Maximum load, D_{max}: Displacement at the P_{max}, P_y: 5% yield load, D_y: Displacement at the P_y, μ: Ductility ratio (D_{max}/D_y)

Theoretical Model

European yield model (EYM)

The theoretical prediction of the strength of the CLT-GLT joint was based on the EYM, as described in Johansen's yield theory (1949). During the theoretical modeling phase, test specimens that did not apply anti-adhesive tape and GFRP rods that did not provide strength characteristics in embedment tests were excluded. In the EYM, the load-carrying capability of the single-lap shear joint fastener was classified into six formulas in Eqs. 6 through 11 based on its unique failure modes:

$$f_{h,1,k} t_1 d \tag{6}$$

$$f_{h,2,k} t_1 d \tag{7}$$

$$\frac{f_{h,1,k} t_1 d}{1+\beta} \left\{ \sqrt{\beta + 2\beta^2 \left[1 + \frac{t_2}{t_1} + \frac{t_2^2}{t_1}\right] - \beta^3 \left(\frac{t_2^2}{t_1}\right)} - \beta\left(1 + \frac{t_2}{t_1}\right) \right\} + \frac{F_{ax,Rk}}{4} \tag{8}$$

$$1.05 \frac{f_{h,1,k} t_1 d}{2+\beta} \left\{ \sqrt{2\beta + 2\beta^2 + \frac{4\beta(2+\beta)M_{y,Rk}}{f_{h,1,k} d t_1^2}} - \beta \right\} + \frac{F_{ax,Rk}}{4} \tag{9}$$

$$1.05 \frac{f_{h,1,k} t_2 d}{1+2\beta} \left\{ \sqrt{2\beta^2 + 2\beta^3 + \frac{4\beta(1+2\beta)M_{y,Rk}}{f_{h,1,k} d t_2^2}} - \beta \right\} + \frac{F_{ax,Rk}}{4} \tag{10}$$

$$1.15 \sqrt{\frac{2\beta}{1+\beta}} \sqrt{2 M_{y,Rk} f_{h,1,k} d} + \frac{F_{ax,Rk}}{4} \tag{11}$$

where $f_{h,1,k}$ is the CLT's embedment strength, $f_{h,2,k}$ is the GLT's embedment strength, t_1 is the CLT's thickness, t_2 is the fastener's penetration depth for the GLT, d is the fastener diameter, β is the ratio of the GLT embedment strength to the CLT embedment strength, and $M_{y,Rk}$ is the fastener's yield moment. The diameter of the fastener was based on the thread root diameter rather than the nominal size. The root diameters of the two types of lag screws were 6.6 mm and 7.7 mm, respectively. The root diameters of fully threaded bolts with diameters of 10 mm and 12 mm were 8.5 mm and 9.6 mm, respectively.

The concept of the rope effect ($F_{ax,Rk}/4$) is to increase the load transfer capacity of the joint by inducing the axial pull-out capacity of the shear fastener, resulting in lateral loading. The rope effect is only considered in the shear fastener yielding mode among the six failure modes. In this study, all fasteners in the joints were perpendicular (90°) to the wood fibers, so the pull-out resistance $F_{ax,Rk}$ based on the type of fastener was calculated using Eq. 12,

$$F_{ax,Rk} = f_{ax,m} d l_{ef} k_d \tag{12}$$

where l_{ef} is the fastener's penetration depth for the GLT. If the fastener diameter is larger than or equal to 8 mm, 1 is applied to k_d. $f_{ax,m}$ is the point side withdrawal strength, which was calculated using the following equation suggested by Eurocode 5 (EN 1995-1-1 2010),

$$f_{ax,m} = 0.52 d^{-0.5} l_{ef}^{-0.1} \rho_m^{0.8} \tag{13}$$

where ρ_m is the GLT's density. The density of the epoxy adhesive, 1170 kg/m³, was applied instead of the density of GLT in the glued-in bolt joints and hybrid joints where the fully threaded bolt penetrated the epoxy pocket of GLT.

Load-carrying capacity $F_{y,exp}$ of the joint by test and strength characteristics derived from the test were substituted into Eqs. 6 through 11 to obtain load-carrying capacity $F_{y,exp,EC5}$. Strength characteristics derived from formulas provided by Eurocode 5 were applied to Eqs. 6 through 11 to compare the modeled load-carrying capacity $F_{y,EC5}$ (Table 7) (EN 1995-1-1 2010). However, the rope effect was calculated using the formula proposed by Eurocode 5 for both $F_{y,exp,EC5}$ and $F_{y,EC5}$ (EN 1995-1-1 2010).

The yield moment of a fastener influences the behavior of the joint. The theoretical formula proposed by Eurocode 5 for predicting the yield moment of fasteners was based on regression analysis using empirical data (EN 1995-1-1 2010). Gečys *et al.* (2019) reported that Eq. 1 based on dynamics is close to the experimentally determined yield moment. $F_{y,exp,EC5}$ was appropriately predicted relative to $F_{y,exp}$. During the actual testing, it appears that the rope effect was adequately demonstrated in the lag screw joint; however, it seemed lacking in the glued-in bolt joint. Therefore, it is necessary to adjust the expected level of the rope effect for the glued-in bolt joint. Further research should be conducted on this matter in the future. The $F_{y,EC5}$ was predicted as approximately 16% higher than the $F_{y,exp}$, which resulted from an overestimation of the yield moment of the estimated fastener. Furthermore, $F_{y,EC5}$ showed a noticeable discrepancy from $F_{y,exp}$ as the rope effect in the glued-in bolt joint was overestimated, as previously mentioned.

Slip Modulus (K_s**)**

K_s was estimated using the Eurocode 5 formula (EN 1995-1-1 2010). The stiffness for one fastener at the joint can be expressed as follows,

$$K_s = \frac{\rho_m^{1.5} d}{23} \tag{14}$$

where $\rho_m = \sqrt{\rho_{m,1} \rho_{m,2}}$ is the average density of timbers. The average density of CLT and GLT was used for the lag screw joint, the density of the adhesive was used for the glued-in bolt joint, and the average density of CLT and adhesive was used for the hybrid joint. The slip coefficient $K_{s,exp}$ for CLT-GLT joints according to the Eurocode 5 formula is

shown in Table 7, along with the experimentally obtained slip coefficient $K_{s,exp}$ (EN 1995-1-1 2010). For the lag screw joint and the hybrid joint, $K_{s,EC5}$ tends to be overestimated compared to $K_{s,exp}$, but it was underestimated in the glued-in bolt joint.

Table 7. Strength Characteristics by Experiment and Test Applied to Eurocode 5 and Load-Carrying Capacity and Slip Modulus According to Eurocode 5

Specimens	$F_{y,exp}$ (kN)	$F_{y,exp,EC5}$ (kN)	$F_{y,EC5}$ (kN)	$k_{s,exp}$ (kN/mm)	$k_{s,EC5}$ (kN/mm)
L10-200	20.4	20.3	22.1	1.2	5.8
L10-250	39.0	35.8	38.9	1.6	5.8
GB10-250	46.6	58.4	61.3	19.7	17.4
GB12-250	68.4	71.7	83.2	27.8	20.9
GG(N)10-250	35.0	-	-	16.7	-
GG(T)12-250	37.1	-	-	10.0	-
HGB10-250	56.7	61.0	67.2	1.85	10.5
*Ratio**	-	5.8%	16.0%	-	-
Note: * Ratio of $F_{y,exp,EC5}$ or $F_{y,EC5}$ relative to $F_{y,exp}$					

CONCLUSIONS

This study conducted push-out tests on the joint parts to evaluate the structural performance of CLT-GLT joints according to lag screw joints, glued-in joints, and hybrid joints. Strength characteristics were determined by material tests, including the bending strength of the fastener and the embedment strength of the timber, and then applied to a theoretical model for comparison with experimental tests. The conclusions drawn from the exam results are as follows:

1. For the glued-in rod joint, it was possible to enhance the reliability of the bonding performance by applying anti-adhesive tape to the bonding surface of the glued-in rod joint. This method was effective in achieving a full composite between the CLT slab and GLT beam. When comparing the glued-in bolt joint to the lag screw joint, it exhibited over 10 times higher slip coefficient and over 2.5 times higher ductility.

2. For the glued-in rod joint, selecting fasteners with high strength contributed to enhancing the strength of the joint. Bonding by fully threaded bolts increased the maximum load on the joint 41% and the slip coefficient 178% compared to bonding by GFRP rods.

3. The hybrid joint, which combines the mechanical joint (CLT part) and glued-in rod joint (GLT part), showed better constructability compared to the glued-in rod joint. The average maximum load was recorded as 47% higher than the lag screw joint and 38% higher than the glued-in bolt joint. However, additional solutions are required to improve the slip coefficient and ductility of this joint.

4. Through the strength characteristics determined by testing, the predicted $F_{y,exp,EC5}$ more accurately predicted the $F_{y,exp}$ from testing than the $F_{y,EC5}$ predicted through the strength characteristics derived from the formulas provided by Eurocode 5. The overestimation of the rope effect and fastener yield moment theoretically estimated at the glued rod joint was attributed to a decrease in the predictive accuracy of the theoretical model for this joint.

ACKNOWLEDGEMENTS

REFERENCES CITED

ASTM D5764-97a (2002). "Standard test method for evaluating dowel-bearing strength of wood and wood-based products," ASTM International, West Conshohocken, PA, USA.

Baek, S. Y., Song, Y. J., Yu, S. H., Kim, D. H., and Hong, S. I. (2021). "Bending performance of cross-laminated timber-concrete composite slabs according to the composite method," *BioResources* 16(4), 8227-8238. DOI: 10.15376/biores.16.4.8227-8238

Chiniforush, A. A., Valipour, H. R., and Ataei, A. (2021). "Timber-timber composite (TTC) connections and beams: An experimental and numerical study," *Construction and Building Materials* 303, article ID 124493. DOI: 10.1016/j.conbuildmat.2021.124493

DIBT (2013). "Würth self-tapping screws," European Technical Approval ETA-11/0190, IfB, Berlin, Germany. (http://www.wuerth.it/download/products/certificazioni_tasse lli/eta_11_0190_eng_2013.pdf).

EN 1995-1-1 (2010). "Design of timber structures - Part 1-1: General - Common rules and rules for buildings," European Committee for Standardization (CEN), Brussels, Belgium.

EN 26891 (1991). "Timber structures, joints made with mechanical fasteners, General principles for the determination of strength and deformation characteristics," European Committee for Standardization (CEN), Brussels, Belgium.

Gečys, T., Bader, T. K., Olsson, A., and Kajėnas, S. (2019). "Influence of the rope effect on the slip curve of laterally loaded, nailed and screwed timber-to-timber connections," *Construction and Building Materials* 228, article ID 116702. DOI: 10.1016/j.conbuildmat.2019.116702

Hammad, M. W., Valipour, H. R., Ghanbari-Ghazijahani, T., and Bradford, M. A. (2022). "Timber-timber composite (TTC) beams subjected to hogging moment," *Construction and Building Materials* 321, article ID 126295. DOI: 10.1016/j.conbuildmat.2021.126295

Hassanieh, A., Valipour, H. R., and Bradford, M. A. (2016). "Load-slip behaviour of steel-cross laminated timber (CLT) composite connections," *Journal of*

Constructional Steel Research 122, 110-121. DOI: 10.1016/j.jcsr.2016.03.008

Hassanieh, A., Valipour, H. R., and Bradford, M. A. (2017a). "Composite connections between CLT slab and steel beam: Experiments and empirical models," *Journal of Constructional Steel Research* 138, 823-836. DOI: 10.1016/j.jcsr.2017.09.002

Hassanieh, A., Valipour, H. R., and Bradford, M. A. (2017b). "Experimental and numerical investigation of short-term behaviour of CLT-steel composite beams," *Engineering Structures* 144, 43-57. DOI: 10.1016/j.engstruct.2017.04.052

Izzi, M., Casagrande, D., Bezzi, S., Pasca, D., Follesa, M., and Tomasi, R. (2018). "Seismic behaviour of cross-laminated timber structures: A state-of-the-art review," *Engineering structures* 170, 42-52. DOI: 10.1016/j.engstruct.2018.05.060

Johansen, K. W. (1949). "Theory of timber connections," *International Association of Bridge and Structural Engineering Publication* 9, 249-262.

KS F 2081 (2021). "Cross laminated timber," Korea Agency for Technology and Standards, Seoul, Korea.

KS F 3021 (2018). "Structural glued laminated timber," Korean Standards Association, Seoul, Korea.

Muñoz, W., Mohammad, M., Salenikovich, A., and Quenneville, P. (2008). "Determination of yield point and ductility of timber assemblies: In search for a harmonised approach," in: *Proceedings of the WCTE*, Miyazaki, Japan, pp. 1-8.

Nie, Y., and Valipour, H. R. (2022). "Experimental and analytical study of timber-timber composite (TTC) beams subjected to long-term loads," *Construction and Building Materials* 342, article ID 128079. DOI: 10.1016/j.conbuildmat.2022.128079

Nie, Y., Karimi-Nobandegani, A., and Valipour, H. R. (2021). "Experimental behaviour and numerical modelling of timber-timber composite (TTC) joints," *Construction and Building Materials* 290, article ID 123273. DOI: 10.1016/j.conbuildmat.2021.123273

Owolabi, D., and Loss, C. (2022). "Experimental and numerical study on the bending response of a prefabricated composite CLT-steel floor module," *Engineering Structures* 260, article ID 114278. DOI: 10.1016/j.engstruct.2022.114278

Sawata, K., and Yasumura, M. (2002). "Determination of embedding strength of wood for dowel-type fasteners," *Journal of Wood Science* 48, 138-146. DOI: 10.1007/BF00767291

Smith, I., Asiz, A., Snow, M., and Chui, Y. H. (2006). "Possible Canadian/ISO approach to deriving design values from test data," in: *39th Meeting of the International Council for Research and Innovation in Building and Construction*, Working Commission W18-Timber Structures, Vol. 28.

Song, Y. J., Baek, S. Y., Yu, S. H., Kim, D. H., and Hong, S. I. (2022). "Evaluation of the bending performance of glued CLT-concrete composite floors based on the CFRP reinforcement ratio," *BioResources* 17(2), 2243-2258. DOI: 10.15376/biores.17.2.2243-2258

Yagi, H., Shioya, S., and Tomiyoshi, E. (2016). "Innovative hybrid timber structures in Japan: Bending behaviour of T-shaped CLT-to-hybrid timber composite beam," in: *Proceedings of the WCTE*, Vienna, Austria, pp. 1-9.

Yasumura, M. (1998). "Estimating seismic performance of wood-framed structures," in: *Proceedings of 5th WCTE*, Montreux, Switzerland, 2, pp. 564-571.

Zhang, C., Zheng, X., and Lam, F. (2023). "Development of composite action in a new long-span timber composite floor: Full-scale experiment and analytical approach," *Engineering Structures* 279, article ID 115550. DOI: 10.1016/j.engstruct.2022.115550